Check for updates

The oxidative degradation of phenol *via in situ* H_2O_2 synthesis using Pd supported Fe-modified ZSM-5 catalysts†

Alba Santos,‡[a] Richard J. Lewis, [iD] ‡*[a] David J. Morgan, [iD] [ab] Thomas E. Davies,[a] Euan Hampton,[c] Paul Gaskin[c] and Graham J. Hutchings [iD] *[a]

The oxidative degradation of organic contaminants *via* the *in situ* synthesis of H_2O_2 from dilute streams of H_2 and O_2 has the potential to significantly reduce the detrimental environmental and health effects associated with the discharge of such pollutants into water bodies, while offering enhanced activity compared to traditional approaches to water treatment. Herein we investigate the efficacy of a series of bifunctional Pd/Fe-ZSM-5 catalysts towards the degradation of phenol, a model wastewater contaminant, where Fe is responsible for the generation of highly reactive oxygen-based species (ROS) from the synthesised H_2O_2. In particular we demonstrate that through control of Fe speciation and Pd oxidation state it is possible to achieve total conversion of phenol and its derivatives, while also making substantial improvements in regard to catalyst stability over previously studied materials.

Introduction

Posing a risk to human and aquatic life the contamination of water bodies with pharmaceutical, petrochemical and agricultural waste streams, in addition to exogenous hormones and dyes is of growing concern.[1] While the use of chlorination is typical in modern water treatment, the large energy demand associated with the production of stoichiometric oxidants, such as NaOCl, and concerns around toxic chemical residues, has prompted interest in alternative routes to water treatment.[2] The use of advanced oxidative processes (AOPs) which utilise ultraviolet irradiation or ozonation in conjunction with H_2O_2 as a means of disinfection is promising, in particular given the high resistance of many organic pollutants to conventional treatments, such as chlorination.[3] However, high energy costs, overall complexity and the need for substantial reactor redesign may hinder their adoption on a large scale for water disinfection.[4]

The use of Fenton-type systems, which combine homogenous Fe species with pre-formed hydrogen peroxide

(H_2O_2) to generate highly reactive oxygen-based radicals,[5] in particular 'OH, has been shown to be both simple and highly effective in the treatment of chemical contaminants, offering increased efficacy compared to either ozonation or irradiation.[4,6] However, the need for separation of both the homogeneous Fe species and the stabilising agents found in commercial H_2O_2 are considerable obstacles for adoption of this route to water treatment.[7,8] The generation of H_2O_2 *in situ* from dilute streams of H_2 and O_2 would negate the serious drawbacks associated with H_2O_2 produced commercially, avoiding the need to transport and store large quantities of highly concentrated stabilised H_2O_2.[9] Likewise, the use of heterogeneous Fenton active metals would overcome the need for costly separation prior to discharge of treated water streams.[10–13] Indeed, we have recently demonstrated the efficacy of coupling the *in situ* production of H_2O_2 with the formation of reactive oxygen species *via* Fentons pathways for numerous chemical transformations,[14–16] in addition to the remediation of phenol,[17] a model waste stream contaminant. However, in the case of our earlier studies into the oxidative degradation of phenol the leaching of the Fe component was found to be of major concern, with the ability of phenol oxidative products, such as oxalic acid, well known to promote the dissolution of immobilised metal species.[18,19] Additionally earlier studies have shown limited ability to fully oxidise the phenolic derivatives, including catechol and benzoquinone, with the presence of such compounds often posing a greater health concern than that of phenol itself.

[a] *Max Planck centre for Fundamental Heterogeneous Catalysis (FUNCAT), Cardiff Catalysis Institute, School of Chemistry, Cardiff University, Main Building, Park Place, Cardiff, CF10 3AT, UK. E-mail: LewisR27@Cardiff.ac.uk, Hutch@cardiff.ac.uk*
[b] *HarwellXPS, Research Complex at Harwell (RCaH), Didcot, OX11 OFA, UK*
[c] *Dŵr Cymru Welsh Water, Pentwyn Road, Nelson, Treharris, CF46 6LY, UK*
† Electronic supplementary information (ESI) available. See DOI: 10.1039/d2cy00283c
‡ These authors contributed equally to this work.

This journal is © The Royal Society of Chemistry 2022

Catal. Sci. Technol., 2022, **12**, 2943–2953 | **2943**

Numerous studies have identified the high efficacy of precious metal catalysts supported on, or encapsulated within zeolitic frameworks towards the direct synthesis of H_2O_2[20–22] and a range of selective oxidative transformations.[23–25] Additionally, the presence of isolated Fe species encapsulated within the framework of such zeolitic materials has been reported to offer high efficacy in the generation of oxygen-based radicals when used in conjunction with H_2O_2, with these materials showing excellent stability under relatively harsh reaction conditions.[26–29]

With these studies in mind, and with an aim to inhibit the leaching of metal species that has been a cause of concern in previous studies[17,18] we now investigate the efficacy of a series of bifunctional 0.5%Pd/Fe-ZSM-5 catalysts, for the oxidative degradation of phenol *via in situ* H_2O_2 production.

Experimental

Catalyst synthesis

Hydrothermal synthesis of Fe-ZSM-5. Fe-ZSM-5 with a $SiO_2 : Al_2O_3$ ratio of (28 : 1) and a Fe content of 0.06–3 wt% have been prepared using a hydrothermal synthesis methodology, with a similar procedure also utilised for the Fe-free analogue. The procedure to produce the 1%Fe-ZSM-5 catalyst is outlined below.

Tetraethylorthosilicate (TEOS, 10.24 g, Alfa Aesar) was added dropwise to a solution of tetrapropylammonium hydroxide 1 M (TPAOH, 15 g, 1.0 M, Merck) and homogenised at 60 °C for 2 hours.

Separately sodium aluminate (0.2901 g, Alfa Aesar) diluted in 5 mL of distilled water and iron nitrate nonahydrate (0.232 g, Alfa Aesar) dissolved in 2.5 mL of distilled water were prepared and added dropwise to the TEOS–TPAOH mixture separately, over the course of 5 minutes. The gel was homogenised (16 h, 60 °C) prior to crystallization in a 200 mL Teflon lined, Parr Instruments stainless-steel autoclave, equipped with pressure relief (72 h, 175 °C). After crystallisation, the resulting solid was filtered and washed with distilled water, until the filtrate reached a neutral pH. The resulting solid was dried (16 h, 70 °C), followed by calcination (flowing air, 550 °C, 3 h, 1 °C min^{-1}).

Subsequently the sample was ion-exchanged with NH_4NO_3 (Merck) (1.0 M, 30 mL g^{-1} of zeolite) three times (100 °C, 4 h), with the suspension filtered and the solid dried (16 h, 70 °C) between each reflux. The sample was activated prior to the impregnation of active metal species (static air, 550 °C, 3 h, 10 °C min^{-1}).

Synthesis of 0.5%Pd/Fe-ZSM-5. The Fe-containing ZSM-5 material was subsequently impregnated with Pd *via* an excess chloride impregnation procedure, based on a methodology previously reported in the literature.[30–32] The procedure to produce 0.5%Pd/1%Fe-ZSM-5 (1 g) is outlined below:

Aqueous acidified $PdCl_2$ solution (0.833 mL, 0.58 M HCl, 6 mg mL^{-1}, Merck) was charged into a 50 mL round-bottom flask and heated to 60 °C with stirring (800 rpm) in a thermostatically controlled oil bath, with total volume fixed to 16 mL using H_2O (HPLC grade, Fischer Scientific). Upon reaching 60 °C, the Fe-ZSM-5 support material (0.995 g) was added over the course of 10 min with constant stirring. The resulting slurry was stirred at 60 °C for a further 15 min, following this the temperature was raised to 95 °C for 16 h to allow for complete evaporation of water. The resulting solid was ground prior to a reductive heat treatment (5%H_2/Ar, 400 °C, 4 h, 10 °C min^{-1}).

Total metal loading of Pd immobilised Fe-ZSM-5 catalysts as determined by ICP-MS analysis of microwave assisted *aqua regia* digestion is reported in Table S1.†

Catalyst testing

Note 1. Reaction conditions used within this study operate below the flammability limits of gaseous mixtures of H_2 and O_2. In all cases reagent gases were not continually introduced into the reactor.

Note 2. The conditions used within this work for H_2O_2 synthesis and degradation have previously been investigated, with the presence of CO_2 as a diluent for reactant gases identified as key to maintaining high catalytic efficacy towards H_2O_2 production.[31,33] Indeed, the effect of CO_2 has been shown to be comparable to that achieved through the addition of HNO_3 to the reaction solution, so that the pH was reduced to a value of 4.[34] However, unlike the use of halo- or oxo-acid stabilisers the formation of carbonic acid *in situ* would not neccessitate additional costly seperation steps.

Note 3. All pressures are given as gauge pressures. In all cases reaction temperature was controlled using a HAAKE K50 bath/circulator using an appropriate coolant.

Direct synthesis of H_2O_2

Hydrogen peroxide synthesis was evaluated using a Parr Instruments stainless steel autoclave with a nominal volume of 50 mL, equipped with a glass liner so that nominal volume is reduced to 33 mL, and a maximum working pressure of 2000 psi. To test each catalyst for H_2O_2 synthesis, the autoclave liner was charged with catalyst (0.01 g) and solvent (8.5 g H_2O, HPLC Grade, Fischer Scientific). The charged autoclave was then purged three times with 5% H_2/CO_2 (100 psi) before filling with 5% H_2/CO_2 (420 psi), followed by the addition of 25% O_2/CO_2 (160 psi). The pressure of 5% H_2/CO_2 and 25% O_2/CO_2 are given as gauge pressures. The reaction was conducted at a temperature of 30 °C, typically for 0.5 h with stirring (1200 rpm). H_2O_2 productivity was determined by titrating aliquots of the final solution after reaction with acidified $Ce(SO_4)_2$ (0.0085 M) in the presence of ferroin indicator. Catalyst productivities are reported as $mol_{H_2O_2}kg_{cat}^{-1}$ h^{-1}.

Degradation of H_2O_2

Catalytic activity towards H_2O_2 degradation (*via* hydrogenation and decomposition pathways) was determined in a similar manner to that used to measure the direct synthesis activity of a catalyst. The autoclave liner was

2944 | *Catal. Sci. Technol.*, 2022, **12**, 2943–2953

This journal is © The Royal Society of Chemistry 2022

charged with water (7.82 g, HPLC grade, Fischer Scientific), H_2O_2 (50 wt% 0.68 g, Merck), and catalyst (0.01 g), with the solvent composition equivalent to a 4 wt% H_2O_2 solution. From the solution 2 aliquots of 0.05 g were removed and titrated with acidified $Ce(SO_4)_2$ solution using ferroin as an indicator to determine an accurate concentration of H_2O_2 at the start of the reaction. The autoclave was purged three times with 5% H_2/CO_2 (100 psi) before filling with 5% H_2/CO_2 to a gauge pressure of 420 psi. The reaction was conducted at a temperature of 30 °C, for 0.5 h with stirring (1200 rpm). After the reaction was complete the catalyst was removed from the reaction mixture *via* filtration and two aliquots of 0.05 g were titrated against the acidified $Ce(SO_4)_2$ solution using ferroin as an indicator. The catalytic activity towards H_2O_2 activity is reported as $mol_{H_2O_2} kg_{cat}^{-1} h^{-1}$.

Oxidative degradation of phenol *via* the *in situ* production of H_2O_2

Catalytic activity towards the degradation of phenol was evaluated using a Parr Instruments stainless steel autoclave with a nominal volume of 50 mL, equipped with a PTFE liner so that nominal volume is reduced to 33 mL, and a maximum working pressure of 2000 psi. In a typical test the autoclave was charged with catalyst (0.01 g) and phenol (8.5 g, 1000 ppm aqueous phenol). The charged autoclave was then purged three times with 5% H_2/CO_2 (100 psi) before filling with 5% H_2/CO_2 to a pressure of 420 psi, followed by the addition of 25% O_2/CO_2 (160 psi). Pressure of 5% H_2/CO_2 and 25% O_2/CO_2 are given as gauge pressures. The reactor was then heated to 30 °C followed by stirring (1200 rpm) typically for 1 h. After 1 h gas mixtures were sampled and analysed *via* GC (Varian 3800 GC fitted with TCD and equipped with a Porapak Q column). The reaction solution was collected and catalyst removed *via* filtration, the post-reaction solution was analysed by high performance liquid chromatography (HPLC) fitted with an Agilent Poroshell 120 SB-C18 column.

Throughout product distribution is of phenol oxidation have been grouped into two categories, namely phenol oxygenated derivatives (including hydroquinone, catechol, *para*-benzoquinone and resorcinol) and organic acids (including muconic acid, maleic acid, oxalic acid, malonic acid, oxalic acid, formic acid and acetic acid). While it was possible to delineate between many of the phenolic derivatives our analysis was unable to clearly identify the individual organic acids. As such selectivity to these species was determined based on phenol conversion and formation of the phenolic derivatives. While it is theoretically possible for the complete oxidation of phenol to occur, the presence of water as a reaction medium and carbon dioxide as a reagent gas diluent prevents the detection of these total oxidation products. As such we are unable to determine the extent to which these final oxidative products are formed (if at all). If these species

are produced during the phenol oxidation reaction they will be encompassed within the selectivity towards organic acids. The oxidative degradation products of phenol are presented in Fig. S1.†

Phenol conversion (eqn (1)), H_2 conversion (eqn (2)) and selectivity towards phenolic derivatives (eqn (3)) or organic acids (eqn (4)) are defined as follows:

$$\text{Phenol Conversion (\%)} = \frac{\text{mmol}_{\text{phenol}(t(0))} - \text{mmol}_{\text{phenol}(t(1))}}{\text{mmol}_{\text{phenol}(t(0))}} \times 100$$

$$(1)$$

$$\text{H}_2 \text{ Conversion (\%)} = \frac{\text{mmol}_{\text{H}_2(t(0))} - \text{mmol}_{\text{H}_2(t(1))}}{\text{mmol}_{\text{H}_2(t(0))}} \times 100 \quad (2)$$

$$\text{Selectivity}_{\text{phenolic derivitives}} (\%) \quad (3)$$
$$= \frac{\text{Phenolic derivitives observed (mmol)}}{\text{Phenol consumed (mmol)}} \times 100$$

$$\text{Selectivity}_{\text{organic acids}} (\%) = \frac{\text{mmol}_{\text{phenol}(t(1))} - \text{mmol}_{\text{phenol derivatives}(t(1))}}{\text{mmol}_{\text{phenol}(t(0))}}$$

$$(4)$$

Gas replacement experiments for the oxidative degradation of phenol *via* the *in situ* production of H_2O_2

An identical procedure to that outlined above for the degradation of phenol was followed for a reaction time of 2 h. After this, stirring was stopped and the reactant gas mixture vented, prior to replacement with the standard pressures of 5% H_2/CO_2 (420 psi) and 25% O_2/CO_2 (160 psi). The reaction mixture was then stirred (1200 rpm) for a further 2 h at 30 °C. To collect a series of data points, as in the case of Fig. 3, it should be noted that individual experiments were carried out and the reactant mixture was not sampled on-line.

Catalyst reusability for the oxidative degradation of the oxidation of phenol *via* the *in situ* production of H_2O_2

In order to determine catalyst reusability, a similar procedure to that outlined above for the oxidative degradation of phenol *via in situ* H_2O_2 production is followed utilising 0.05 g of catalyst. Following the initial test, the catalyst was recovered by filtration and dried (30 °C, 16 h, under vacuum); from the recovered catalyst sample 0.01 g was used to conduct a standard phenol degradation experiment.

Hot filtration experiments for the oxidative degradation of the oxidation of phenol *via* the *in situ* production of H_2O_2

An identical procedure to that outlined above for the oxidative degradation of phenol was followed for a reaction time of 1 h. Following this, the stirring was stopped, and the reactant gas mixture vented prior to the removal of the solid catalyst *via* filtration. The post-
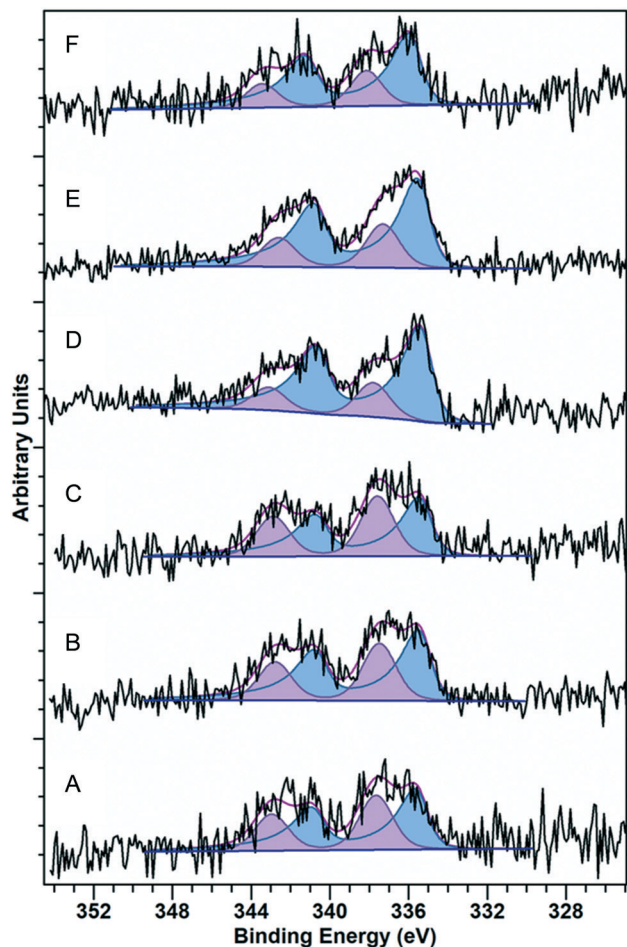
This journal is © The Royal Society of Chemistry 2022

Catal. Sci. Technol., 2022, **12**, 2943–2953 | **2945**

Fig. 1 Pd(3d) core-level spectra for (A) 0.5%Pd/ZSM-5 (B) 0.5%Pd/0.06%Fe-ZSM-5, (C) 0.5%Pd/0.1%Fe/ZSM-5, (D) 0.5%Pd/0.5%Fe/ZSM-5, (E) 0.5%Pd/1%Fe-ZSM-5 and (F) 0.5%Pd/3%Fe-ZSM-5. Key: Pd^0 (blue), Pd^{II} (purple). Note: all samples exposed to reductive heat treatment (4 h, 500 °C, 10 °C min^{-1}, 5%H_2/Ar).

reaction solution was returned to the reactor to identify the contribution of leached species to the observed activity. Further experiments were conducted, where a fresh 0.5%Pd/ZSM-5 catalyst (0.01 g) or pre-formed H_2O_2 (at concentrations comparable to if all the H_2 in a standard *in situ* experiment was selectively converted), was added to the reaction mixture prior to running the reaction for a further 1 h.

Note 4. It should be noted that it was not possible to measure residual H_2O_2 *via* standard titration or colorimetric procedures given the strong reddish colour that results from the formation of the aromatic oxidation products (catechol, hydroquinone *etc.*).

Note 5. In all cases reactions were run multiple times, over multiple batches of catalyst, with the data being presented as an average of these experiments. The catalytic activity toward the direct synthesis and subsequent degradation of H_2O_2 as well as the oxidative degradation of phenol was found to be consistent to within ±2% on the basis of multiple reactions.

Catalyst characterisation

X-ray photoelectron spectroscopy (XPS) was performed on a Thermo Fisher Scientific K-alpha$^+$ spectrometer. Samples were analysed using a micro-focused monochromatic Al X-ray source (72 W) using the "400-micron spot" mode, which provides an analysis defining elliptical X-ray spot of *ca.* 400 × 600 microns. Data was recorded at pass energies of 150 eV for survey scans and 40 eV for high resolution scan with 1 eV and 0.1 eV step sizes respectively. Charge neutralisation of the sample was achieved using a combination of both low energy electrons and argon ions.

Data analysis was performed in CasaXPS v2.3.24[35] after calibrating the data to Si(2p) peak taken to have a value of 103.5 eV. Quantification was made using a Shirley type background and Scofield cross sections, with an electron energy dependence of −0.6.

The bulk structure of the catalysts was determined by powder X-ray diffraction using a (θ–θ) PANalytical X'pert Pro powder diffractometer using a Cu K_α radiation source, operating at 40 KeV and 40 mA. Standard analysis was carried out using a 40 min run with a back filled sample, between 2θ values of 10–80°. Phase identification was carried out using the International Centre for Diffraction Data (ICDD). Sample crystallinity was determined based on a commercial HZSM-5 material (Zeolyst, SiO_2 : Al_2O_3 = 23), using the intensity of the of the peaks 2θ = 22–25°.

Fourier-transform infrared spectroscopy (FTIR) was conducted using a Bruker Tensor 27 spectrometer, fitted with a HgCdTe (MCT) detector and operated with OPUS software.

Transmission electron microscopy (TEM) was performed on a JEOL JEM-2100 operating at 200 kV. Samples were prepared by dispersion in ethanol by sonication and deposited on 300 mesh copper grids coated with holey carbon film. Energy dispersive X-ray analysis (EDX) was performed using an Oxford Instruments X-Max^N 80 detector and the data analysed using the Aztec software.

To allow for quantification of total metal loading catalysts were digested *via* an *aqua regia* assisted, microwave digestion method using a Milestone Connect Ethos UP microwave with an SK15 sample rotor. Digested samples were analysed using an Agilent 7900 ICP-MS equipped with I-AS auto-sampler. All samples were diluted by a factor of 10 using HPLC grade H_2O (1% HNO_3 and 0.5% HCl matrix). All calibrants were matrix matched and measured against a five-point calibration using certified reference materials purchased from Perkin Elmer and certified internal standards acquired from Agilent.

Metal leaching from catalyst supported was quantified using microwave plasma-atomic emission spectroscopy (MP-AES). Metal concentrations were determined by response at two characteristic emissions wavelengths for Fe (372.0 nm, 259.9 nm) and Pd (340.5 nm, 363.5 nm) and the resultant concentrations averaged. The concentration response of Fe and Pd were calibrated using commercial reference standards (Agilent), in all cases r^2 > 0.999.
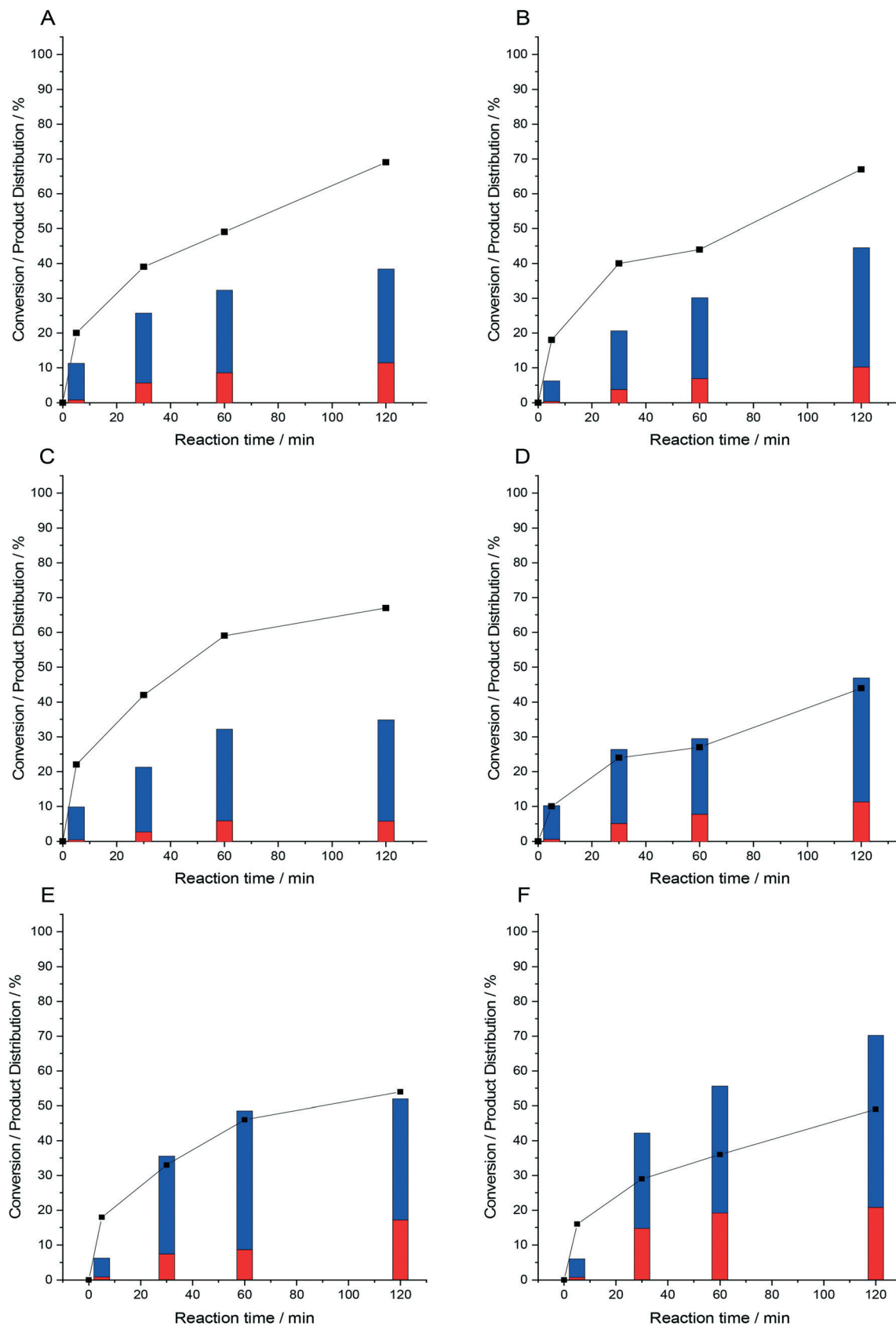
2946 | *Catal. Sci. Technol.*, 2022, **12**, 2943–2953

This journal is © The Royal Society of Chemistry 2022

Fig. 2 Comparison of the catalytic activity toward the oxidative degradation of phenol *via in situ* H_2O_2 synthesis as a function of reaction time over. (A) 0.5%Pd/ZSM-5, (B) 0.5%Pd/0.06%Fe-ZSM-5, (C) 0.5%Pd/0.125%Fe-ZSM-5, (D) 0.5%Pd/0.5%Fe-ZSM-5, (E) 0.5%Pd/1%Fe-ZSM-5 and (F) 0.5%Pd/3%Fe-ZSM-5. Key: selectivity towards phenolic derivatives (red bar), selectivity towards organic acids (blue bar), H_2 conversion (black squares). Phenol oxidation reaction conditions: catalyst (0.01 g), phenol (1000 ppm), 5% H_2/CO_2 (420 psi), 25% O_2/CO_2 (160 psi),1200 rpm, 30 °C.
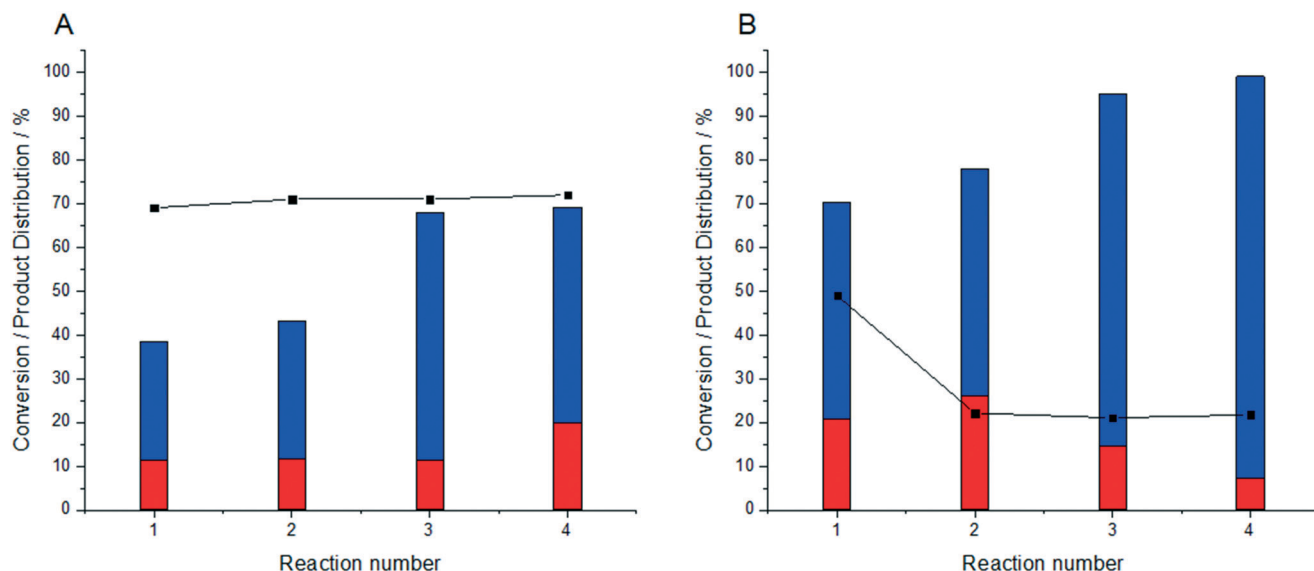
Fig. 3 Comparison of the catalytic activity toward the oxidative degradation of phenol *via in situ* H_2O_2 synthesis over sequential reaction number. (A) 0.5%Pd/ZSM-5, (B) 0.5%Pd/3%Fe-ZSM-5. Key: selectivity towards phenolic derivatives (red bar), selectivity towards organic acids (blue bar), H_2 conversion (black squares). Phenol oxidation reaction conditions: catalyst (0.01 g), phenol (1000 ppm), 5% H_2/CO_2 (420 psi), 25% O_2/CO_2 (160 psi), 1200 rpm, 30 °C.

N_2 isotherms were collected on a Micromeritics 3-Flex. Samples (*ca.* 0.070 g) were degassed (350 °C, 9 h) prior to analysis. Analyses were carried out at 77 K with P_0 measured continuously. Free space was measured post-analysis with He. Data analysis was carried out using the Micromeritics 3-Flex software, using the non-local density functional theory (NLDFT), Tarazona model.

Results and discussion

Our initial studies *via* UV-vis spectroscopy established the successful incorporation of Fe (0.06–0.5 wt%) into the zeolitic framework (Fig. S2 and Note S1†). The incorporated Fe is considered to be present as Fe^{3+} tetrahedrally coordinated within the ZSM-5 lattice, in addition to isolated and binuclear Fe species immobilised within the zeolitic framework channels, as evidenced by the presence of reflectance bands between 200–250 and 250–350 nm in all Fe-containing samples. However, in the case of those samples with high Fe content (3 wt%) the observation of reflectance bands above 450 nm also indicates the presence of extra-framework Fe_xO_y particles (clusters and agglomerates) in addition to framework Fe species observed in the materials with lower Fe loadings.[36]

Subsequent FTIR (Fig. S3 and Note S2†) analysis indicated that the introduction of Fe into the MFI framework of ZSM-5 in addition to Pd deposition resulted in no significant detrimental effects on zeolitic structure, as evidenced by comparison to a commercially available Fe-free ZSM-5 analogue.[21] However, further investigation *via* XRD (Fig. S4 and Note S3†) established that there was indeed a minor loss in crystallinity, particularly at higher Fe loadings, which is in keeping with previous studies into metal loaded zeolites.[20,21]

Notably we do not observe any reflections associated with immobilised metals, which may be indicative of high metal dispersion. The details of the textural properties of the synthesised Pd/Fe-ZSM-5 are summarised in Table S2.† In keeping with previous studies,[20] the introduction of the active metals led to a general decrease in both total surface area and pore volume in comparison to the bare ZSM-5 support, with this ascribed to the deposition of metal nanoparticles inside the zeolitic pore structure.

Our initial testing established the efficacy of the Fe-ZSM-5-supported Pd catalysts towards the direct synthesis of H_2O_2 from molecular H_2 and O_2, under conditions considered to be detrimental towards H_2O_2 stability, but relevant to real world application (Table 1).[31] Despite these challenging conditions all catalysts were observed to synthesise H_2O_2, although net H_2O_2 concentrations are clearly limited.

Perhaps unexpectedly, given the ability of Fe to catalyse H_2O_2 degradation to water *via* Fenton's pathways and the strong correlation between Fe content and H_2O_2 degradation activity, increasing Fe incorporation was not found to deleteriously effect H_2O_2 synthesis rates, with the concentration of H_2O_2 achieved over the 0.5%Pd/3%Fe-ZSM-5 catalyst (0.016 wt%) double that of the Fe-free 0.5%Pd/ZSM-5 analogue (0.008 wt%), this is in keeping with our previous studies into supported PdFe catalysts[14] and may result from the differences in reaction conditions utilised to probe both reaction pathways. This is despite a clear correlation between catalytic activity towards H_2O_2 degradation and Fe content, which is attributed to the presence of larger quantities of extra-framework Fe, as evidenced by our analysis *via* UV-vis (Fig. S2†).

We next investigated the effect of Fe incorporation on the efficacy of ZSM-5-supported Pd catalysts towards the oxidative

2948 | *Catal. Sci. Technol.*, 2022, **12**, 2943–2953

This journal is © The Royal Society of Chemistry 2022

Table 1 Catalytic activity of 0.5%Pd/Fe-ZSM-5 catalysts towards the direct synthesis and subsequent degradation of H_2O_2, as a function of total Fe incorporation

Catalyst	Productivity/$mol_{H_2O_2}kg_{cat}^{-1} h^{-1}$	H_2O_2/wt%	Degradation/%
ZSM-5	0	0	0
0.5%Fe-ZSM-5	0	0	1
0.5%Pd/ZSM-5	4	0.008	12
0.5%Pd/0.06%Fe-ZSM-5	4	0.008	18
0.5%Pd/0.125%Fe-ZSM-5	6	0.009	19
0.5%Pd/0.5%Fe-ZSM-5	6	0.011	21
0.5%Pd/1%Fe-ZSM-5	7	0.012	31
0.5%Pd/3%Fe-ZSM-5	8	0.016	41

H_2O_2 direct synthesis reaction conditions: catalyst (0.01 g), H_2O (8.5 g), 5% H_2/CO_2 (420 psi), 25% O_2/CO_2 (160 psi),1200 rpm, 30 °C, 0.5 h.
H_2O_2 degradation reaction conditions: catalyst (0.01 g), H_2O_2 (50 wt%, 0.68 g) H_2O (7.72 g), 5% H_2/CO_2 (420 psi), 1200 rpm, 30 °C, 0.5 h.

degradation of phenol *via in situ* H_2O_2 production (Table 2). A stark divide in catalyst performance was observed, with the Fe-rich catalysts (0.5%Pd/1%Fe-ZSM-5 and 0.5%Pd/3%Fe-ZSM-5) offering significantly higher rates of phenol conversion than the lower Fe loaded analogues. Indeed, little difference in performance was observed for those catalysts that have less than 0.5%Fe incorporated into the zeolite, with low Fe-loaded catalysts achieving approximately 30% phenol conversion over a standard 1 h reaction, which is comparable to that observed over the Fe-free analogue (0.5%Pd/ZSM-5). These observations when coupled with our UV-vis analysis (Fig. S2†) can be considered to be indicative of the role of extra-framework Fe in achieving high rates of phenol conversion.

Subsequent studies, over an extended reaction time established the requirement for both Pd and Fe to be immobilised on the same support grain (Fig. S5†) with the activity of the 0.5%Pd/0.5%Fe-ZSM-5 catalyst (47% phenol conversion) far superior to that of a physical mixture of the 0.5%Pd/ZSM-5 and 0.5%Fe-ZSM-5 catalysts (32% phenol conversion), when using an identical metal concentration to that used in the bi-metallic analogue. The significant improvement in phenol conversion in the presence of H_2 and O_2 in comparison to that observed when using either molecular H_2 or O_2 alone, or indeed an identical concentration of pre-formed H_2O_2 (22% phenol conversion) should also be noted (Fig. S6†). The relatively high rate of phenol conversion observed under a reductive atmosphere (5%H_2/CO_2) is attributed to the presence of dissolved O_2 in

the aqueous phenol solution rather than the formation of phenol hydrogenation products, such as cyclohexanol and cyclohexanone. Indeed, while numerous studies have identified the ability of supported Pd surfaces to catalyse the hydrogenation of phenol, temperatures far exceeding those used within the work are typically required[37] and we have previously ruled out this route to phenol conversion under identical reaction conditions.[18]

The catalytic selectivity of Pd-based catalysts toward H_2O_2 is known to be highly dependent on the oxidation state of Pd, with Pd^0 species typically more active toward both the direct synthesis and subsequent degradation of H_2O_2 than analogous Pd^{2+} materials.[38] Analysis of the Pd-based catalysts *via* X-ray photoelectron spectroscopy (XPS) (Fig. 1, corresponding XP spectra for Fe(2p) region shown in Fig. S7† and atomic ratios reported in Table S3†) reveals that despite exposure to a reductive heat treatment (4 h, 500 °C, 10 °C min^{-1}, 5%H_2/Ar), the surface speciation of the monometallic Pd catalyst consists of a comparable concentration of Pd^0 and Pd^{2+}. However, upon the incorporation of Fe a substantial shift in Pd oxidation state was observed, with the proportion of Pd^0 increasing significantly. With Pd speciation well reported to be a key criterion in determining catalytic performance towards H_2O_2 synthesis, it is therefore possible, at least in part, to attribute the enhanced phenol degradation activity of the Fe containing catalysts to the modification of Pd oxidation state and a resulting increase in H_2O_2 synthesis activity. Notably the performance of the higher Fe-loaded catalysts (0.5%Pd/1%FeZSM-5 and 0.5%Pd/3%FeZSM-5) was

Table 2 Catalytic activity of 0.5%Pd/Fe-ZSM-5 catalysts towards the oxidative degradation of phenol *via in situ* H_2O_2 synthesis, as a function of total Fe incorporation

Catalyst	Phenol conversion/%	Selectivity to phenolic derivatives/%	Selectivity to organic acids/%
ZSM-5	0.0	0.0	0.0
0.5%Fe-ZSM-5	0.0	0.0	0.0
0.5%Pd/ZSM-5	32.0	26.0	74.0
0.5%Pd/0.06%Fe-ZSM-5	30.0	23.0	77.0
0.5%Pd/0.125%Fe-ZSM-5	32.0	18.0	82.0
0.5%Pd/0.5%Fe-ZSM-5	29.0	26.0	74.0
0.5%Pd/1%Fe-ZSM-5	49.0	18.0	82.0
0.5%Pd/3%Fe-ZSM-5	56.0	35.0	65.0

Phenol oxidation reaction conditions: catalyst (0.01 g), phenol (1000 ppm), 5% H_2/CO_2 (420 psi), 25% O_2/CO_2 (160 psi),1200 rpm, 30 °C, 1 h.

found to be far superior to the 0.5%Pd–0.5%Fe/TiO$_2$ catalyst, which we have previously investigated for the oxidative degradation of phenol (39% phenol conversion and 31% selectivity towards the phenol derivatives), under identical reaction conditions.[18] We ascribe this, at least in-part, to the increased proportion of Pd^0 in the materials studied within this work, with a predominance of Pd^{2+} observed in the TiO$_2$ supported materials.

Time-on-line studies comparing the catalytic efficacy of the Fe-ZSM-5-supported Pd catalysts towards the oxidative degradation of phenol can be seen in Fig. 2. As with our standard reaction time studies (1 h), the higher activity of the 0.5%Pd/3%Fe-ZSM-5 catalyst is once again clear, with 70% phenol conversion achieved over a time period of 2 h. Interestingly, regardless of Fe-content the formation of organic acids was observed to be favoured. This is particularly noteworthy given that a number of the phenolic derivatives are considered to be far more toxic than phenol itself[39] and the chemical oxygen demand (an indicative measure of how easily a target molecule is fully oxidised) of the organic acids is far lower than that of the phenolic derivatives, as such the formation of di-acids is clearly preferable in comparison to the less oxidised phenolic derivatives.[40] Further evaluation of catalytic performance towards the direct synthesis of H$_2$O$_2$, under reaction conditions identical to those used for the *in situ* oxidative degradation of phenol and over an identical reaction time (2 h) indicates that generally catalytic performance towards H$_2$O$_2$ formation is not deleteriously affected by the introduction of Fe (Fig. S8†). Indeed, with the exception of the 0.5%Pd/3%Fe-ZSM-5 catalyst we observe that a steady state of H$_2$O$_2$ production can be reached, with the decreased in H$_2$O$_2$ concentration achieved over the 0.5%Pd/3%Fe-ZSM-5 catalyst at extended reaction time attributed to the increased activity of this catalyst to generate both reactive oxygen species and water from H$_2$O$_2$, which correlates well with the improved activity of this catalyst towards the oxidative degradation of phenol and the high rates of H$_2$O$_2$ degradation previously reported (Table 1).

The observed plateau in phenol conversion rate observed over many of the catalysts (Fig. 2), although notably not the 0.5%Pd/3%Fe-ZSM-5 catalyst, may be indicative of the deactivation of the catalyst at relatively long reaction times. This is of particular concern given the ability of the di-acids generated during the degradation of phenol to catalyse the leaching of active metals.[19] Alternatively, the relatively high H$_2$ conversion rates observed over all catalysts at extended reaction times (Fig. 2), may be indicative of the reaction instead becoming limited by H$_2$ availability. This can be understood through the first order dependence of H$_2$O$_2$ production with respect to H$_2$[41] and in turn the limited generation of reactive oxygen species, which are responsible for phenol degradation, when H$_2$ availability is limited.

To determine the cause for the loss in catalytic performance over the course of the phenol degradation

reaction and with a focus on the 0.5%Pd/ZSM-5 and 0.5%Pd/3%Fe-ZSM-5 catalysts (mean particle size distributions, as determined by TEM analysis of the fresh materials are reported in Fig. S9†), we next conducted a series of sequential phenol oxidation experiments, where reagent gases were replenished at 2 h intervals (Fig. 3). The enhanced activity of the 0.5%Pd/3%Fe-ZSM-5 catalyst is once again clear, with a near total phenol conversion achieved over four sequential experiments (99% phenol conversion), far greater than that observed over the 0.5%Pd/ZSM-5 analogue (70% phenol conversion) over the same number of reactions. Indeed, even over three successive reactions the 0.5%Pd/3%Fe-ZSM-5 catalyst is able to achieve near total conversion of phenol (95%). Perhaps more importantly, the product distribution observed over the 0.5%Pd/3%Fe-ZSM-5 catalyst is observed to shift significantly towards the formation of organic acids (92% selectivity) after 4 successive reactions. This is a major improvement over our earlier work into PdFe/TiO$_2$ catalysts, with these previously investigated materials unable to achieve comparable rates of phenol conversion or direct product distribution substantially towards the less toxic organic acids.[18]

Determination of H$_2$ conversion rates over the sequential phenol degradation reactions is indicative of the stability of the 0.5%Pd/ZSM-5 catalyst, with approximately 70% H$_2$ conversion observed for each successive reaction. However, the lower rates of both phenol conversion and selectivity towards the organic acids should also be noted. While the rate of H$_2$ conversion over the 0.5%Pd/3%Fe-ZSM-5 catalyst in the initial phenol oxidation reaction (49%) is considerably lower than that of the 0.5%Pd/ZSM-5 catalyst, which is indicative of a more selective utilisation of the gaseous reagent, this metric is not maintained upon further sequential reactions. Although it should be noted that H$_2$ conversion does reach a steady value after the initial reaction, with approximately 20% H$_2$ conversion observed upon in subsequent reactions. This may be indicative of the catalyst reaching a more stable activity.

For any heterogeneous catalyst operating in a three-phase system the possibility of the leaching of active metals and resulting homogeneous contribution to observed catalytic performance is of great concern, with homogeneous Pd and Fe species known to catalyse the direct synthesis of H$_2$O$_2$ and subsequent Fenton's reaction respectively.[41–43] Indeed, we have previously reported significant Fe leaching (>45%) during the oxidative degradation of phenol, under identical reaction conditions, when utilising a PdFe/TiO$_2$ catalyst, with the presence of the further phenol oxidation products identified to be key in catalysing metal leaching.[17,18] Analysis of post reaction solutions *via* microwave plasma atomic emission spectroscopy (MP-AES) (Table S4†) reveals a significant improvement in catalyst stability compared to our earlier works and clearly demonstrates the key role of the zeolite support in inhibiting metal loss, this is despite the much greater selectivity of the zeolite based catalysts to species known to promote metal leaching.[19] We attribute the improved stability of the Pd/Fe-ZSM-5 catalysts studied within

2950 | *Catal. Sci. Technol.*, 2022, **12**, 2943–2953

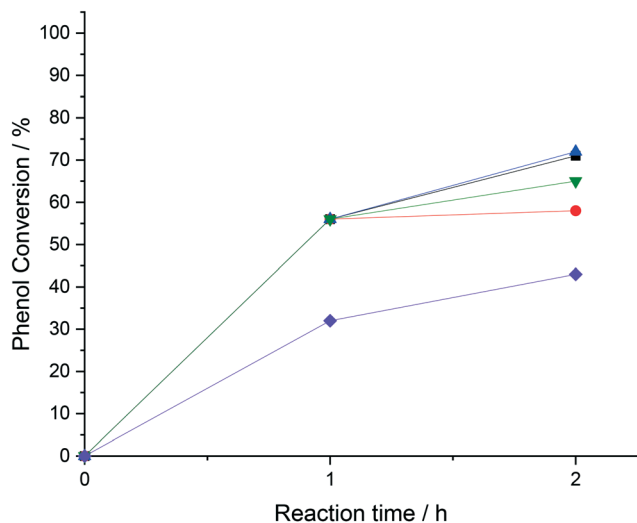This journal is © The Royal Society of Chemistry 2022

Fig. 4 Efficacy of leached species in oxidative degradation of phenol as identified by a hot filtration experiment using the 0.5%Pd/3%Fe-ZSM-5 catalyst. Phenol oxidation reaction conditions: catalyst (0.01 g), phenol (1000 ppm), 5% H_2/CO_2 (420 psi), 25% O_2/CO_2 (160 psi),1200 rpm, 2 h, 30 °C. Key: 0.5%Pd/3%Fe-ZSM-5 catalysed reaction (black squares); 0.5%Pd/ZSM-5 catalysed reaction (purple diamonds); hot filtration reaction where the 0.5%Pd/3%Fe-ZSM-5 catalyst is removed by filtration after 1 h (red circles); hot filtration reaction where 0.5%Pd/3%Fe-ZSM-5 catalyst removed by filtration after 1 h and replaced by 0.5%Pd/ZSM-5 catalyst for final 1 h of reaction (blue triangles); hot filtration reaction where 0.5%Pd/3%Fe-ZSM-5 catalyst removed by filtration after 1 h and H_2O_2 is added to the reaction (inverted green triangles). Note: in the case of the experiment using commercial H_2O_2 the second half of the reaction was carried out under an atmosphere of 25%O_2/CO_2 (580 psi).

this work, in comparrison to those previously studied for the oxidative degradation of phenol, to the incorporation of large quantities of Fe into the zeoltitic framework. As evidenced by our earlier UV-vis analysis (Fig. S2†), which reveled the presence of extra-framework Fe nanoparticles at only very high Fe loadings (>3 wt% Fe).

With a particular focus on the 0.5%Pd/3%Fe-ZSM-5 catalyst, we next conducted a series of hot-filtration experiments to identify the contribution of leached metal species to catalytic activity (Fig. 4, corresponding product distribution reported in Table S5†). In the absence of the solid catalyst, minimal additional phenol conversion was observed (58%), after the two-part, 2 h duration experiment. This value was nearly identical to that observed for the 0.5%Pd/3%Fe-ZSM-5 catalyst over a 1 h reaction (56%), with

the limited additional conversion of phenol possibly attributed to the contribution from residual H_2O_2 generated in the initial 1 h reaction.

To determine if the inactivity observed in the 0.5%Pd/3%Fe-ZSM-5 hot-filtration experiment was due to the limited ability of the homogeneous component to synthesize H_2O_2, a further hot-filtration experiment was conducted whereby, after the initial 1 h reaction, the 0.5%Pd/3%Fe-ZSM-5 catalyst was replaced with a 0.5%Pd/ZSM-5 catalyst, ensuring that the total moles of Pd was equal to that in the 0.5%Pd/3%Fe-ZSM-5 catalyst. Perhaps unexpectedly, given the activity of the 0.5%Pd/ZSM-5 catalyst towards the oxidative degradation of phenol (Table 2) an increase in this metric was observed (72%), somewhat similar to the sum of the 0.5%Pd/3%Fe-ZSM-5 (56%) and 0.5%Pd/ZSM-5 (32%) components when they were used independently over 1 h. Indeed, the extent of phenol conversion was found to be identical to that observed over the analogous two-part, 2 h duration experiment conducted over the 0.5%Pd/3%Fe-ZSM-5 catalyst alone (72%). Given the ability of the 0.5%Pd/ZSM-5 catalyst to promote the degradation of phenol this experiment was unable to confirm a contribution from homogeneous Fe species. In a final experiment, after the initial 1 h reaction utilising the 0.5%Pd/3%Fe-ZSM-5 catalyst alone, commercial H_2O_2, at a concentration equivalent to if all H_2 in the phenol degradation reaction was selectively converted to H_2O_2 was added to the reaction mixture. After a further 1 h reaction (carried out in the presence of an atmosphere of O_2/CO_2) a small increase in phenol conversion was observed (65%). When coupled with the known ability of homogenous Fe species to catalyse the formation of oxygen based radical species, *via* the Fenton process, and the presence of small quantities of Fe in the post-reaction solution (Table S4†) this may be indicative of a homogenous component. However, if a homogeneous component to the oxidative degradation of phenol does exist, we consider that these hot filtration experiments, in addition to those earlier studies that illustrated the need for close contact between species responsible for H_2O_2 synthesis and subsequent activation to oxygen-based radicals to indicate that such a contribution is minimal.

Finally, in an attempt to increase phenol conversion and drive product distribution further down the oxidative pathway towards the less toxic di-acids the total mass of the 0.5%Pd/3%Fe-ZSM-5 catalyst used in the oxidative degradation of phenol was increased (Table 3). With

Table 3 Catalytic performance towards the oxidative degradation of phenol *via in situ* H_2O_2 synthesis, as a function of catalyst mass

Catalyst	Catalyst mass/g	Phenol conversion/%	Selectivity towards phenolic derivatives/%	Selectivity towards organic acids/%
0.5%Pd/3%Fe-ZSM-5	0.01	70	29	71
	0.02	97	19	81
	0.03	100	0	100
	0.04	100	0	100

Phenol oxidation reaction conditions: catalyst (0.01–0.04 g), phenol (1000 ppm), 5% H_2/CO_2 (420 psi), 25% O_2/CO_2 (160 psi),1200 rpm, 2 h, 30 °C.

This journal is © The Royal Society of Chemistry 2022

Catal. Sci. Technol., 2022, **12**, 2943–2953 | **2951**

complete phenol conversion and selectivity towards organic acids observed when using 0.03 g of the catalyst, further highlighting the efficacy of the *in situ* approach to phenol degradation.

Conclusion

In conclusion we have demonstrated the efficacy of Pd supported Fe-incorporated ZSM-5 catalysts towards the oxidative degradation of phenol *via in situ* H_2O_2 synthesis. This is observed using conditions where conversion is limited using commercial H_2O_2. The presence of extra-framework Fe is shown to be crucial in promoting catalytic performance, with the optimal 0.5%Pd/3%Fe-ZSM-5 catalyst achieving significantly greater rates of phenol conversion and selectivity towards less toxic products than the Fe-free analogue. Additionally, these materials demonstrate a significant improvement in both stability and performance, compared to the previously studied oxide support PdFe materials. We consider that they represent a promising avenue for future research, particularly for application in total oxidative degradation of a range of chemical pollutants.

Conflicts of interest

The authors declare no conflict of interest.

Acknowledgements

References

1 S. B. Grant, J. Saphores, D. L. Feldman, A. J. Hamilton, T. D. Fletcher, P. L. M. Cook, M. Stewardson, B. F. Sanders, L. A. Levin, R. F. Ambrose, A. Deletic, R. Brown, S. C. Jiang, D. Rosso, W. J. Cooper and I. Marusic, *Science*, 2012, **337**, 681–686.

2 T. Richards, J. H. Harrhy, R. J. Lewis, A. G. R. Howe, G. M. Suldecki, A. Folli, D. J. Morgan, T. E. Davies, E. J. Loveridge, D. A. Crole, J. K. Edwards, P. Gaskin, C. J. Kiely, Q. He, D. M. Murphy, J. Maillard, S. J. Freakley and G. J. Hutchings, *Nat. Catal.*, 2021, **4**, 575–585.

3 H. Li, X. Zhu and J. Ni, *Electrochim. Acta*, 2011, **56**, 9789–9796.

4 S. Esplugas, J. Giménez, S. Contreras, E. Pascual and M. Rodríguez, *Water Res.*, 2002, **36**, 1034–1042.

5 H. J. H. Fenton, *J. Chem. Soc., Trans.*, 1894, **65**, 899–910.

6 J. J. Pignatello, E. Oliveros and A. MacKay, *Crit. Rev. Environ. Sci. Technol.*, 2006, **36**, 1–84.

7 J. R. Scoville and I. A. Novicova (Cottrell Ltd.), US5900256, 1996.

8 P. Wegner, US20050065052A1, 2003.

9 R. J. Lewis and G. J. Hutchings, *ChemCatChem*, 2019, **11**, 298–308.

10 F. Martínez, G. Calleja, J. A. Melero and R. Molina, *Appl. Catal., B*, 2005, **60**, 181–190.

11 R. Liou, S. Chen, M. Hung, C. Hsu and J. Lai, *Chemosphere*, 2005, **59**, 117–125.

12 S. Queirós, V. Morais, C. S. D. Rodrigues, F. J. Maldonado-Hódar and L. M. Madeira, *Sep. Purif. Technol.*, 2015, **141**, 235–245.

13 Y. Yan, X. Wu and H. Zhang, *Sep. Purif. Technol.*, 2016, **171**, 52–61.

14 C. M. Crombie, R. J. Lewis, R. L. Taylor, D. J. Morgan, T. E. Davies, A. Folli, D. M. Murphy, J. K. Edwards, J. Qi, H. Jiang, C. J. Kiely, X. Liu, M. S. Skjøth-Rasmussen and G. J. Hutchings, *ACS Catal.*, 2021, **11**, 2701–2714.

15 C. M. Crombie, R. J. Lewis, D. Kovačič, D. J. Morgan, T. J. A. Slater, T. E. Davies, J. K. Edwards, M. S. Skjøth-Rasmussen and G. J. Hutchings, *Catal. Lett.*, 2021, **151**, 2762–2774.

16 R. Underhill, M. Douthwaite, R. J. Lewis, P. J. Miedziak, R. D. Armstrong, D. J. Morgan, S. J. Freakley, T. Davies, A. Folli, D. M. Murphy, Q. He, O. Akdim, J. K. Edwards and G. J. Hutchings, *Res. Chem. Intermed.*, 2021, **47**, 303–324.

17 R. Underhill, R. J. Lewis, S. J. Freakley, M. Douthwaite, P. J. Miedziak, J. K. Edwards, O. Akdim and G. J. Hutchings, *Johnson Matthey Technol. Rev.*, 2018, **62**, 417–425.

18 A. Santos, R. J. Lewis, D. J. Morgan, T. E. Davies, E. Hampton, P. Gaskin and G. J. Hutchings, *Catal. Sci. Technol.*, 2021, **11**, 7866–7874.

19 S. O. Lee, T. Tran, Y. Y. Park, S. J. Kim and M. J. Kim, *Int. J. Miner. Process.*, 2006, **80**, 144–152.

20 R. J. Lewis, K. Ueura, Y. Fukuta, S. J. Freakley, L. Kang, R. Wang, Q. He, J. K. Edwards, D. J. Morgan, Y. Yamamoto and G. J. Hutchings, *ChemCatChem*, 2019, **11**, 1673–1680.

21 R. J. Lewis, A. Bara-Estaun, N. Agarwal, S. J. Freakley, D. J. Morgan and G. J. Hutchings, *Catal. Lett.*, 2019, **149**, 3066–3075.

22 Z. Jin, Y. Liu, L. Wang, C. Wang, Z. Wu, Q. Zhu, L. Wang and F. Xiao, *ACS Catal.*, 2021, **11**, 1946–1951.

23 G. Li, J. Edwards, A. F. Carley and G. J. Hutchings, *Catal. Commun.*, 2007, **8**, 247–250.

24 G. Li, D. I. Enache, J. Edwards, A. F. Carley, D. W. Knight and G. J. Hutchings, *Catal. Lett.*, 2006, **110**, 7–13.

25 Z. Jin, L. Wang, E. Zuidema, K. Mondal, M. Zhang, J. Zhang, C. Wang, X. Meng, H. Yang, C. Mesters and F. Xiao, *Science*, 2020, **367**, 193–197.

26 C. Hammod, M. M. Forde, M. H. Ab Rahim, A. Tetford, Q. He, R. L. Jenkins, N. Dimitratos, J. A. Lopez-Sanchez, N. F. Dummer, D. M. Murphy, A. F. Carley, S. H. Taylor, D. J. Willock, E. E. Strangland, J. Kang, H. Hagen, C. J. Kiely and G. J. Hutchings, *Angew. Chem., Int. Ed.*, 2012, **51**, 5129–5133.

27 C. Hammond, R. L. Jenkins, N. Dimitratos, J. A. Lopez-Sanchez, M. H. Ab Rahim, M. M. Forde, A. Thetford, D. M. Murphy, H. Hagen, E. E. Strangland, J. M. Moulijn, S. H.

2952 | *Catal. Sci. Technol.*, 2022, **12**, 2943–2953

This journal is © The Royal Society of Chemistry 2022

Taylor, D. J. Willock and G. J. Jutchings, *Chem. – Eur. J.*, 2012, **18**, 15735–15745.

28 M. M. Forde, R. D. Armstrong, C. Hammond, Q. He, R. L. Jenkins, S. A. Kondrat, N. Dimitratos, J. A. Lopez-Sanchez, S. H. Taylor, D. Willock, C. J. Kiely and G. J. Hutchings, *J. Am. Chem. Soc.*, 2013, **135**, 11087–11099.

29 C. Kalamaras, D. Palomas, R. Bos, A. Horton, M. Crimmin and K. Hellgardt, *Catal. Lett.*, 2016, **146**, 483–492.

30 M. Sankar, Q. He, M. Morad, J. Pritchard, S. J. Freakley, J. K. Edwards, S. H. Taylor, D. J. Morgan, A. F. Carley, D. W. Knight, C. J. Kiely and G. J. Hutchings, *ACS Nano*, 2012, **6**, 6600–6613.

31 A. Santos, R. J. Lewis, G. Malta, A. G. R. Howe, D. J. Morgan, E. Hampton, P. Gaskin and G. J. Hutchings, *Ind. Eng. Chem. Res.*, 2019, **58**, 12623–12631.

32 J. Brehm, R. J. Lewis, D. J. Morgan, T. E. Davies and G. J. Hutchings, *Catal. Lett.*, 2021, **152**, 254–262.

33 D. A. Crole, R. Underhill, J. K. Edwards, G. Shaw, S. J. Freakley, G. J. Hutchings and R. J. Lewis, *Philos. Trans. R. Soc., A*, 2020, **378**, 20200062.

34 J. K. Edwards, A. Thomas, A. F. Carley, A. A. Herzing, C. J. Kiely and G. J. Hutchings, *Green Chem.*, 2008, **10**, 388–394.

35 N. Fairley, V. Fernandez, M. Richard-Plouet, C. Guillot-Deudon, J. Walton, E. Smith, D. Flahaut, M. Greiner, M. Biesinger, S. Tougaard, D. Morgan and J. Baltrusaitis, *Appl. Surf. Sci.*, 2021, **5**, 100112.

36 J. Xu, R. D. Armstrong, G. Shaw, N. F. Dummer, S. J. Freakley, S. H. Taylor and G. J. Hutchings, *Catal. Today*, 2016, **270**, 93–100.

37 H. Zhou, B. Han, T. Liu, X. Zhong, G. Zhuang and J. Wang, *Green Chem.*, 2017, **19**, 3585–3594.

38 V. R. Choudhary, A. G. Gaikwad and S. D. Sansare, *Catal. Lett.*, 2002, **83**, 235–239.

39 Z. Wu and M. Zhou, *Environ. Sci. Technol.*, 2001, **35**, 2698–2703.

40 A. A. Aghapour, G. Moussavi and K. Yaghmaeian, *J. Environ. Manage.*, 2015, **157**, 262–266.

41 Q. Liu and J. H. Lunsford, *Appl. Catal., A*, 2006, **314**, 94–100.

42 V. Kavitha and K. Palanivelu, *Int. J. Environ. Sci. Technol.*, 2016, **13**, 927–936.

43 V. Kavitha and K. Palanivelu, *Chemosphere*, 2004, **55**, 1235–1243.

This journal is © The Royal Society of Chemistry 2022

Catal. Sci. Technol., 2022, **12**, 2943–2953 | **2953**